Cancer Therapy: Clinical

Clinical Cancer Research

Population Analysis of Erlotinib in Adults and Children Reveals Pharmacokinetic Characteristics as the Main Factor Explaining Tolerance Particularities in Children

Melanie White-Koning[1], Elodie Civade[1], Birgit Geoerger[2], Fabienne Thomas[1], Marie-Cécile Le Deley[3], Isabelle Hennebelle[1], Jean-Pierre Delord[1], Etienne Chatelut[1], and Gilles Vassal[2]

Abstract

Purpose: The aim of this pharmacokinetic–pharmacodynamic (PK–PD) analysis was to evaluate the pharmacologic characteristics of erlotinib and its main metabolite (OSI-420) in pediatric patients compared with those in adult patients.

Experimental Design: Plasma concentrations of erlotinib and OSI-420 of 46 children with malignant brain tumors included in a phase I study and 42 adults with head and neck carcinoma were analyzed by a population-pharmacokinetic method (NONMEM). The effect of several covariates and single nucleotide polymorphisms (SNP) in *ABCB1*, *ABCG2*, and *CYP3A5* on pharmacokinetic parameters was evaluated. PK/PD relationships between plasma drug exposure Area Under the Curve (AUC) at day 1 and skin toxicity were studied in children and compared with the relationship observed in adults.

Results: A significant difference in erlotinib clearance ($P = 0.0001$), when expressed in $L{\cdot}h^{-1}{\cdot}kg^{-1}$, was observed between children and adults with mean values of 0.146 and 0.095, respectively (mean difference = 0.051 $L{\cdot}h^{-1}{\cdot}kg^{-1}$, SD = 0.0594). However, a common covariate model was obtained describing erlotinib clearance according to body weight, alanine aminotransferase, *ABCB1*, and *CYP3A5* polymorphisms (*2677*G > T/A and *6986*G > A) for both children and adult patients. The PK–PD relationship was very consistent between the children and adult groups with risk of skin toxicity rising with increasing erlotinib AUC.

Conclusions: The nonlinear population approach applied to pharmacokinetic data combined with a pharmacokinetic–pharmacodynamic analysis revealed that the higher recommended dose in children (125 mg/m^2/day) compared with adults (90 mg/m^2/day) is mainly due to pharmacokinetic rather than pharmacodynamic particularities. *Clin Cancer Res; 17(14); 4862–71. ©2011 AACR.*

Introduction

Erlotinib (Tarceva) is an orally active, potent, and selective inhibitor of the epithelial growth factor receptor (EGFR) tyrosine kinase. From a pharmacokinetic point of view, erlotinib is metabolized by CYP3A4, CYP3A5, CYP1A1, and CYP1A2 isoforms of the P450 enzyme (1). The main active metabolite OSI-420 is produced by O-demethylation of the side chains and represents approximately 5% of the circulating erlotinib (2). It has been suggested that erlotinib is a substrate of both ABCB1 (P-glycoprotein) and ABCG2 (BCRP) transporters (3, 4). Erlotinib is registered for treatment of locally advanced or metastatic nonsmall cell lung cancer with stable disease after standard platinum-based first-line chemotherapy or after failure of at least one prior chemotherapy regimen, according to a daily dose of 150 mg per day (5). Erlotinib is also indicated at a daily dose of 100 mg in combination with gemcitabine for the treatment of patients with metastatic pancreatic cancer (6). Several promising preclinical studies have led to the exploration of its use in pediatrics, particularly in children with malignant brain tumors overexpressing EGFR (7, 8). Broniscer and colleagues reported on erlotinib pharmacokinetics in plasma of an 8-year old child with glioblastoma treated with oral erlotinib and found it to be similar to that of published adult studies (9). A Phase I study was set up with 46 children with refractory solid tumors treated with erlotinib alone or erlotinib and temozolomide (10). The authors determined that the maximum tolerated dose (MTD) was 85 mg/m^2/day, however significant interpatient variability in erlotinib disposition was also found at all dose

Authors' Affiliations: [1]EA4553, Institut Claudius Regaud et Université de Toulouse, France; [2]Department of Pediatric and Adolescent Oncology, Centre National de Recherche Scientifique UMR8203; Vectorology and Anticancer Therapeutics, Université Paris-Sud 11, Institut Gustave Roussy; and [3]Biostatistics and Epidemiology, Université Paris-Sud 11, Institut Gustave Roussy, Villejuif, France

Note: M. White-Koning and E. Civade have contributed equally to this work.

Corresponding Author: Etienne Chatelut, Institut Claudius-Regaud, 20–24, rue du Pont St Pierre, 31052 Toulouse cedex – France. Phone: +33-5-61-42-42-71; E-mail: chatelut.etienne@claudiusregaud.fr

doi: 10.1158/1078-0432.CCR-10-3278

Translational Relevance

Erlotinib is an oral epithelial growth factor receptor (EGFR) tyrosine kinase inhibitor approved for treatment of lung and pancreas cancers with potential applications in pediatrics particularly for the treatment of malignant brain tumors overexpressing EGFR. The recommended erlotinib dose differs between pediatric and adult patients (125 mg/m^2/day versus 90 mg/m^2/day, respectively).

The reason for this difference must be examined to compare the erlotinib therapeutic index in children and in adults, and to identify additional causes of interindividual pharmacokinetic or pharmacodynamic variability.

By using a population pharmacokinetic approach to simultaneously analyze data from two clinical trials (i.e., neoadjuvant pilot study in adults with head and neck carcinoma and phase 1 study in pediatrics), we show that the difference is related to pharmacokinetics, and not to the pharmacokinetic–pharmacodynamic relationship.

These results are useful not only for the clinical use of erlotinib, but also in terms of methodology to encourage future analysis of combined data from children and adults.

levels. Another Phase I study in 23 patients with high-grade glioma aged 3 to 22 including erlotinib pharmacokinetics administered concurrently with radiotherapy found a much higher MTD of 120/mg/m^2/day (11). The authors found that the PK variables of erlotinib and OSI-420 were similar to those described in adults. A third multicenter phase I study was carried out to establish the recommended dose of erlotinib, when given alone or combined with radiotherapy to children with malignant brain tumors (12). The recommended dose (125 mg/m^2/day) was found to be the same for both treatment strata and is higher than that in adults (corresponding to around 90 mg/m^2/day). The dosing of tyrosine kinase inhibitors has become an issue. Relationships between imatinib dose and efficacy have been observed in some subgroups of patients with gastrointestinal stromal tumors (GIST) defined according to c-Kit genotype (13). However Delbaldo and colleagues found a wide dispersion of imatinib plasma concentrations in 34 patients with advanced GIST receiving the same dose, with no relationship between imatinib exposure and response rate or between total or free unbound imatinib and clinical activity, but a positive correlation between exposure and hematologic toxicity (14). Other studies described close relationships between plasma imatinib concentrations and both efficacy and toxicity in patients with either chronic myeloid leukemia (15, 16) or GIST (17, 18). Similar relationships have been observed for sunitinib (19).

The aim of this pharmacokinetic–pharmacodynamic (PK–PD) analysis was to evaluate the pharmacologic characteristics of erlotinib in paediatric patients compared with those in adult patients. The adult pharmacokinetic data was provided by a neoadjuvant pilot study carried out in patients with head and neck carcinoma (20, 21) and the pediatric data come from a phase 1 study in children with malignant brain-tumors (12). First, both datasets were combined to evaluate PK characteristics. Secondly, relationships between individual pharmacokinetic parameters, such as erlotinib plasma exposure, and adverse events were examined to compare child and adult patients' pharmacodynamic sensitivity to the drug.

Patients and Methods

Patients

Adult patients ($n = 42$) with nonmetastatic head and neck tumors awaiting surgical resection were enrolled in a clinical trial. The study design and eligibility criteria have been described previously in detail (20). Patients were treated with erlotinib at 150 mg/day for a variable period corresponding to the time between pan-endoscopy and surgical resection. In the event of grade 2 or more diarrhea or skin rash that were symptomatically unacceptable to the patient, treatment was withheld until resolution to grade 1, and then erlotinib was restarted at a dose of 100 mg/day. If toxicity reoccurred, erlotinib was stopped.

Fifty young patients (age range 2 to 19 years) with malignant brain tumors were included within a multicenter, dose escalation phase I study (NCT00418327; ITCC-003/MO18461) of the Innovative Therapies with Children with Cancer (ITCC) European Consortium. Children with histologically/cytologically confirmed malignant brain tumors refractory to, or relapsing after, first line therapy, for which no effective treatment exists, were enrolled into Group 1 (erlotinib alone). Children with newly diagnosed, histologically confirmed brainstem glioma were enrolled into Group 2 (erlotinib and radiotherapy). Eligibility criteria are described in the article reporting the clinical results (12). Erlotinib tablets were administered orally once daily in 3-week cycles at four dose levels; 1 = 75 mg/m^2, 2 = 100 mg/m^2, 3 = 125 mg/m^2, 4 = 150 mg/m^2. According to the recommendations for the conduct of phase I trials in children with cancer (22), the starting dose was approximately 80% of the adult recommended dose (RD) (150 mg/day). In Group 2, patients received local irradiation to the brainstem region of 54 Gy over 6 weeks (1.8 Gy/fraction/day). The first erlotinib dose was administered within 4 hours of the first irradiation. Conventional 3+3 dose escalation methodology was used for Group 1 (23), with an extension of 10 patients at the RD. In Group 2, dose escalation decisions were made using a continual reassessment method with likelihood-based inference (24).

Both populations of patients (adults and children) were fasted when taking the drug as recommended in the protocols. For both children and adults, complete medical histories, a physical examination, and the following laboratory tests were done at baseline and at each scheduled visit: complete differential blood count, albumin (ALB), α1 acid glycoprotein (AGP), alanine aminotransaminase (ALAT).

The concomitant administration of enzymatic inducers (such as carbamazepine, phenytoin, and glucocorticoids) was also reported in both populations. Both studies were approved by independent institutional review board/ethical committees and conducted in compliance with the Declaration of Helsinki and the Guidelines for Good Clinical Practice. Written informed consent was obtained from all subjects or parents/legal representatives in the case of children under 18.

Pharmacokinetic Study

Blood sampling and mass spectrometry analysis

Serial blood samples were taken at various intervals to determine the pharmacokinetic profile of erlotinib and its principal metabolite (OSI-420). For adults, on day 1 of the treatment, three blood samples were collected from each patient: before erlotinib administration, 2 hours and 4 to 8 hours after the dose. Patients were clinically evaluated at a median time of 14 days after starting the treatment and one blood sample 24 hours after the last administration was obtained. On the day preceding, and the day of the surgery, two additional samples were collected (6–8 hours and approximately 24 hours, respectively, after the last administration of erlotinib).

For children and young adults, plasma samples were collected before drug intake at day 1, 30 minutes, 1, 2, 4, 6, 8, and 24 hours after the erlotinib dose at day 8 and day 22 for group 1 and at day 8 and day 43 (end of irradiation) for group 2.

For both children and adults, blood samples were centrifuged (1500 g, 15 min, 4°C), the plasma frozen at −20°C until analysis and the determination of plasma erlotinib and OSI-420 was done by Advion BioServices, Inc (Ithaca). Quantitative analyses were done using a validated coupled liquid chromatography-mass spectrometry technique (25). The calibration range was 1–3000 ng/ml for erlotinib and 1–1000 ng/ml for OSI-420.

Genetic analysis

A blood sample was collected on day 1 for pharmacogenetic investigation. Genomic DNA was extracted from peripheral blood leukocytes according to standard procedures with QIAamp DNA Blood Mini Kit (Qiagen) according to the manufacturer's instructions. Genotyping was done for 5 single-nucleotide polymorphisms (SNP). *ABCB1* variants (*2677*G>T, *2677*G>A and *3435*C>T) were determined by PCR-RFLP as previously described (26, 27). *ABCG2 421*C>A variant was determined by polymerase chain reaction (PCR) and direct sequencing as published before (21). The presence of *CYP3A5*1/CYP3A5*3* alleles was determined on genomic DNA with allele specific real time PCR as previously described (28). Whenever genetic data was missing, genotypes were randomly assigned according to the frequency of the genotypes in the remaining study population. Box plots of clearance values were examined to verify that this attribution did not change the population clearance distribution.

Population pharmacokinetic analysis

Plasma erlotinib and OSI-420 concentrations were analyzed according to a nonlinear mixed effects approach using the NONMEM program (version VI, level 1.0, Icon Development Solutions running on an Intel Core 2 Quad) according to a one-compartment pharmacokinetic model for erlotinib and to a two-compartment pharmacokinetic model when both erlotinib and OSI-420 were analyzed and using the first-order conditional estimation (FOCE) method (21). A proportional error model was used for both interpatient and residual variability.

Determination of individual pharmacokinetic parameters and covariate analyses

The influence of the following variables on pharmacokinetic parameters was examined: body weight, sex (0 for male, 1 for female), age, population (coded POP = 0 for adults and POP = 1 for children), albuminemia, plasma AGP level, ALAT concentration, effect of simultaneous administration of enzymatic inducers (carbamazepine, phenytoine, dexamethasone, prednisone, prednisolone), genotype for *ABCB1* (*2677*G>T/A and *3435*C>T), *ABCG2* (*421*C > A) and *CYP3A5* (*6986*G > A). Moreover, interoccasion variability (IOV) was tested on all the parameters because data from 2 cycles were analyzed simultaneously. The first occasion was defined as the samples of cycle 1 (i.e., day 1 and day 8 for children) and the second occasion as those of cycle 2 (i.e., day 22 for group 1 patients) or cycle 3 (i.e. day 43 for group 2 patients). There was no IOV for adults because they only received one cycle of erlotinib.

First, the influence of each covariate on total plasma clearance of erlotinib (CL) was tested individually. For example, in the case of body weight, the following equation was used: $CL = \theta 1\ (WT/\text{mean WT})^{\theta 2}$, where $\theta 1$ is the typical value of CL (TVCL) estimated by the population mean and $\theta 2$ is the estimated influential factor for body weight. The χ^2 test was used to compare the objective function values (OFV = −2loglikelihood) of nested models (likelihood ratio test). A decrease of at least 3.84 ($P < 0.05$) was required for a covariate to be considered significantly correlated with the pharmacokinetic variable. Second, an intermediate model including all significant covariates was obtained. A stepwise backward elimination procedure was carried out. Covariates remained in the final population pharmacokinetic model when the removal of the covariate resulted in an increase of the OFV of at least 10.83 ($P < 0.001$). The influence of covariates on other pharmacokinetic parameters (volume of distribution V and absorption constant Ka) was examined using the same methodology. The likelihood ratio test was also used to select the structural pharmacokinetic model. Once the population pharmacokinetics model for erlotinib had been defined (including the covariates), all the parameter values were fixed while developing the OSI-420 pharmacokinetic model using the same methodology as described for erlotinib. A bioavailability (F) of 1 was assumed in the absence of IV drug administration data and CL and V corresponded to apparent parameters (i.e., CL/F and V/F).

Performance of final pharmacokinetic model

A visual predictive check (VPC) was carried out by simulating from the final model 1000 concentrations post-dose at day 1, day 8, day 22, and 43. The 50th percentile concentration (as an estimator of the population-predicted concentration) and the 5th and 95th percentile concentrations were processed using R (RfN, version 2007a) and then plotted with Stata version 10.0, Stata Co.

Pharmacokinetic/Pharmacodynamic relationship

Systemic exposure to erlotinib was calculated using individual post hoc clearance: AUC = dose/CL for erlotinib. Relationship between AUC at day 1 (i.e., dose/CL at day 1) and skin toxicity at the midterm treatment visit was evaluated in children and was compared with the relationship previously observed in adults (21). Toxicity (i.e., skin rash, folliculitis, acne, and pruritis) was evaluated at the midterm treatment visit and graded using the National Cancer Institute Common Toxicity Criteria, version 2.0 or 3.0. The relationship between initial daily AUC and skin toxicity grade was examined using a four-level ordered logistic regression for adults (with skin toxicity graded 0–3) and using a three-level ordered logistic regression for children [with skin toxicity graded 0, 1 and 2/3 (grades 2 and 3 were grouped as only 3 children developed a grade 3 skin toxicity)]. Based on this model, the cumulative-predicted probabilities of skin toxicity according to AUC were obtained and represented as curves. The analyses were conducted using Stata version 10.0, Stata Co.

Determination of cutoff point of erlotinib AUC

Receiver operating characteristic (ROC) curves were constructed to examine the value of an erlotinib AUC threshold predicting a minimum skin toxicity of grade 2. The area under ROC curves of erlotinib AUC both in children and in adults for the prediction of a minimum skin toxicity of grade 2 were calculated. The diagnostic accuracy values of sensitivity (SE) and specificity (SP) were determined. The optimal cutoff value was obtained. The analyses were conducted using Stata version 10.0, Stata Co.

Results

Patients

Forty-two adults were assessable for pharmacokinetic investigations and plasma samples of 46 children (26 in group 1 and 20 in group 2) were analyzed. A total of 1659 plasma samples were taken into account for the population pharmacokinetic analysis. Adults were treated for a median time of 20 days (range 5–32 days) and children for 50 days (range 8–106 days). Complete pharmacogenetic data were available for 79 (42 adults and 37 children) of the 88 patients. Minor allele frequencies are given in Table 1 (footnote). The genotypes did not depart significantly from Hardy–Weinberg equilibrium (exact tests nonsignificant in all four cases $P > 0.10$). The patients' characteristics at baseline are summarized in Table 1.

Determination of individual pharmacokinetic parameters and covariate analyses

Erlotinib pharmacokinetics were adequately described by a one-compartment model with first-order absorption and first-order elimination. The corresponding pharmacokinetic variables were CL/F (apparent total plasma clearance of erlotinib), V/F (apparent volume of distribution of erlotinib), and Ka (absorption rate constant). The pharmacokinetic model included interoccasion variability of CL/F and V/F. During the individual testing of the 11 covariates, 7 covariates [body weight, population variable coded POP indicating whether patient is a child or an adult ALAT concentration, *ABCB1 2677*G > T/A and *3435*C > T, *ABCG2 421*C > A, and *CYP3A5*1* allele] were significantly ($P < 0.05$) associated with clearance. However, sex, albuminemia, plasma AGP level, and effect of simultaneous administration of enzymatic inducers were not found to be significantly associated with clearance. A stepwise backward elimination applied to the intermediate model identified the following covariates as remaining significant ($P < 0.001$): body weight, ALAT concentration, *CYP3A5*1*, and *ABCB1* (*2677*G > T/A). An increase in body weight was associated with an increase in CL (positive θ coefficient) whereas an increase in ALAT concentration led to a decrease in CL (negative θ coefficient). For example, CL/F is estimated to increase, on average, by approximately 22% between a typical individual weighing 52 kg and one weighing 72 kg, all other covariates being equal. Concerning the effect of ALAT, CL/F is estimated to decrease, on average, by approximately 19% between a typical individual with ALAT concentration of 24.4 IU/L and one with ALAT concentration of 50 IU/L, all other covariates being equal. The presence of a variant allele of *ABCB1 2677*G > T/A was associated with a 19% decrease in CL whereas the presence of a *CYP3A5*1* allele was associated with a 42% increase in CL. For V/F, body weight was the only significant ($P < 0.001$) covariate associated with a decrease in interindividual variability (IIV) from 56.6% (no covariate) to 13%. The final covariate models are detailed in Table 2. Of note, substantial interoccasion variability was observed for CL/F and V/F (22% and 46%, respectively). The residual variability was 31.9% for erlotinib concentrations.

Analysis of both plasma erlotinib and OSI-420 concentrations required an additional compartment with first order elimination from the metabolite compartment and the corresponding pharmacokinetics parameters: CLm/fm (apparent total clearance of OSI-420) and Vm/fm (apparent volume of distribution of OSI-420), where fm is the fraction of erlotinib converted into OSI-420. Four covariates (body weight, ALB, ALAT, and *ABCB1* (*2677*G > T/A)) were significantly ($P < 0.05$) correlated with CLm/fm. Three covariates [body weight, ALAT, and *ABCB1* (*2677*G>T/A)] remained significant ($P < 0.001$) after the stepwise backward elimination procedure from the intermediate model (Table 2). A sensitivity analysis excluding the 9 patients for which the pharmacogenetic data was incomplete was conducted to test the robustness of the model and all covariates found in the final model remained significant ($P < 0.001$) (data not shown). The proportion of circulating active

Table 1. Summary of patients' characteristics at baseline

	Abbrevation	Children ($n = 46$) Mean (range)	Adults ($n = 42$) Mean (range)	All patients ($n = 88$) Mean (range)
Demographic and morphologic covariates				
Sex (Male/Female)	SEX	19/27	39/3	58/30
Age (years)	AGE	8.8 (2–19)	55.7 (39–83)	31.2 (2–83)
Weight (kg)	WT	32 (14–73)	73.9 (44–110)	52.0 (14–110)
Biological covariates				
Serum Albumin (g/L)	ALB	40.0 (20–50)	37.7 (30–45)	38.9 (20–50)
Alanine aminotransaminase (IU/L)	ALAT	21.6 (6–50)	27.4 (9–86)	24.4 (6–86)
α1 Acid glycoprotein (g/L)	AAG	1.2 (0.63–2.28)	1.0 (0.55–2.3)	1.1 (0.55–2.3)
Genetic covariates (see footnote for minor allele frequencies[a])				
CYP3A5	CYP			
*3/*3		28	38	66
*1/*3		7	4	11
*1/*1		2	0	2
ND[b]		9	0	9
ABCG2 exon *5–C421A*	ABCG2			
CC		39	34	73
CA		2	8	10
AA		0	0	0
ND[b]		5	0	5
ABCB1 exon *26–C3435T*	ABCB1e26			
CC		10	10	20
CT		20	22	42
TT		11	10	21
ND[b]		5	0	5
ABCB1 exon *21–G2677T/A*	ABCB1e21			
GG		13	15	28
GT		19	23	42
GA		2	0	2
TT		7	4	11
AA		0	0	0
AT		0	0	0
ND[b]		5	0	5
Others				
Concomitant administration of enzymatic inducers[c]	IND	11	1	12

[a]minor allele frequencies (excluding ND category): *CYP3A5*1*: 0.09; *ABCG2–421A*: 0.06; *ABCB1–3435T*: 0.51; *ABCB1–2677T*: 0.39 and *A*: 0.01.
[b]ND: not determined.
[c]Carbamazepine, phenytoin, glucocorticoids.

metabolite OSI-420 compared with erlotinib, calculated using AUCmetabolite/(AUCmetabolite + AUCerlotinib), was 8.1% (SD = 3.2%).

About the discrepancy between the recommended doses in adults and children (90 and 125 mg/m^2/day, respectively), the impact of the covariate POP on the pharmacokinetic model was carefully evaluated. The typical value of erlotinib clearance was 27% lower ($P < 0.001$) in children when POP was the only considered covariate, and 24% higher ($P < 0.025$) if POP was considered together with body weight (Table 2). Comparison of the individual POSTHOC values of clearance confirmed these differences: the mean value (± SD) was significantly lower (41%) in children (CL/F = 4.15 ± 2.22 L.h^{-1}) in comparison with that in adults (CL/F = 6.98 ± 3.48 L.h^{-1}) ($P < 0.0001$) while the mean (± SD) weighted clearance value was 54% higher in children (0.146 ± 0.070 L·h^{-1}·kg^{-1} for children versus 0.095 ± 0.045 L·h^{-1}·kg^{-1} for adults, $P = 0.0001$, Student's t-test). However, the addition of the POP covariate to the final covariate model (i.e., the model which

Table 2. Final covariate models for pharmacokinetic parameters and models comparing erlotinib clearance in children and adults

	Coefficient values	95% CI	CV (%)
Final model			
ERLOTINIB: CL/F (L/h) $= \theta_1.(WT/52.0)^{\theta 2}.\theta_3{}^{CYP}.\theta_4{}^{ABCB1e21}.(ALAT/24.4)^{\theta 5}$	V/F (L) $= \theta_6.(WT/52.0)^{\theta 7}$	Ka (h^{-1}) $= \theta_8$	
Apparent clearance (CL/F):	$\theta_1 = 5.17$	(4.33–6.01)	42.1
	$\theta_2 = 0.62$	(0.46–0.78)	
	$\theta_3 = 1.42$	(1.16–1.68)	
	$\theta_4 = 0.81$	(0.67–0.95)	
	$\theta_5 = -0.29$	(–0.44 to –0.15)	
Apparent volume of distribution (V/F):	$\theta_6 = 159$	(135–184)	13.0
	$\theta_7 = 0.74$	(0.53–0.96)	
Absorption rate constant (Ka):	$\theta_8 = 0.94$	(0.65–1.24)	115.3
Interoccasion variability/CL			22
Interoccasion variability/V			46
Residual variability			31.9
OSI 420: CLm/fm (L/h) $= \theta_9.(WT/52.0)^{\theta 10}.\theta_{11}{}^{ABCB1e21}.(ALAT/24.4)^{\theta 12}$	Vm/fm (L) $= \theta_{13}$		
Apparent clearance (CLm/fm):	$\theta_9 = 74.7$	(42.8–107)	53.8
	$\theta_{10} = 0.66$	(0.41–0.92)	
	$\theta_{11} = 0.78$	(0.48–1.07)	
	$\theta_{12} = -0.21$	(–0.48 to 0.06)	
Apparent volume of distribution (Vm/fm)	$\theta_{13} = 15.3$	(1.66–28.9)	94.3
Interoccasion variability/CLm			29.3
Residual variability			39.9
Models with POP covariate			
		θ^{POP} value	ΔOFV
$CL/F = \theta_1.\theta_2{}^{POP}$		$\theta_2 = 0.73$ (0.58–0.88)	–20 ($P < 0.001$)
$CL/F = \theta_1.(WT/52.0)^{\theta 2}.\theta_3{}^{POP}$		$\theta_3 = 1.24$ (0.84–1.64)	–6.1 ($P < 0.025$)
$CL/F = \theta_1.(WT/52.0)^{\theta 2}.\theta_3{}^{CYP}.\theta_4{}^{ABCB1e21}.(ALAT/24.4)^{\theta 5}.\theta_6{}^{POP}$		$\theta_6 = 1.11$ (0.86–1.36)	–1.2 (NS)

Abbreviations: CV, coefficient of variation for inter-individual variability (not explained by the covariable, if any) or residual variability;Δ OFV, change in objective function value (OFV) by comparison with the corresponding model without covariate POP; CYP 3A5 = 0 for homozygous **3/*3* patients and CYP 3A5 = 1 for heterozygous **3/*1* or homozygous **1/*1* patients; ABCB1e21 = 0 for wild-type patients (*2677GG*) and ABCB1e21 = 1 for heterozygous (*2677GT* or *2677GA*) or homozygous variant-type (*2677 TT*) patients; NS, Not significant; POP = 0 for adults, POP = 1 for children.

includes body weight, ALAT, *CYP3A5*, and *ABCB1* (*2677*G>T/A)) did not significantly decrease the OFV, and the exponent corresponding to POP was only 1.11 (Table 2). Moreover, when the child population was split between children (age < 12 years; $n = 35$) and adolescents (age ≥ 12 years; $n = 11$), the mean weighted clearance of adolescents (i.e., 0.099 ± 0.056 $L.h^{-1}.kg^{-1}$) was significantly ($P = 0.009$) lower than that of children (0.161 ± 0.068 $L.h^{-1}.kg^{-1}$) but not significantly different from the adults' weighted clearance (0.095 ± 0.045 $L.h^{-1}.kg^{-1}$). All these results indicate that although erlotinib clearance differs between children and adults, the final covariate model explains most of this difference.

Performance of final pharmacokinetic model

This final model adequately described erlotinib and OSI-420 pharmacokinetic profiles as shown by the goodness-of-fit plots (Fig. 1) and by the VPC (Fig. 2).

Pharmacokinetic/Pharmacodynamic relationships

The relationship between drug exposure and the severity of skin toxicity was examined. The box plot in Fig. 3 shows an increase in AUC with increasing grade of toxicity in both children and adults. This positive association between exposure and toxicity was significant in the four-level ordered logistic regression analysis for adults ($P = 0.014$; ref. 13) and a trend is observed in the three-level ordered logistic regression analysis for children ($P = 0.06$). Figure 4 shows the cumulative probabilities of having skin toxicity according to AUC using the probabilities predicted by the ordered logistic regression models [adult data analyzed with the model previously published (13) and children data analyzed with the present model]. There is within each population, adults or children, a strong PK/PD relationship, which seems very similar. It is noteworthy that skin toxicity was not significantly correlated with

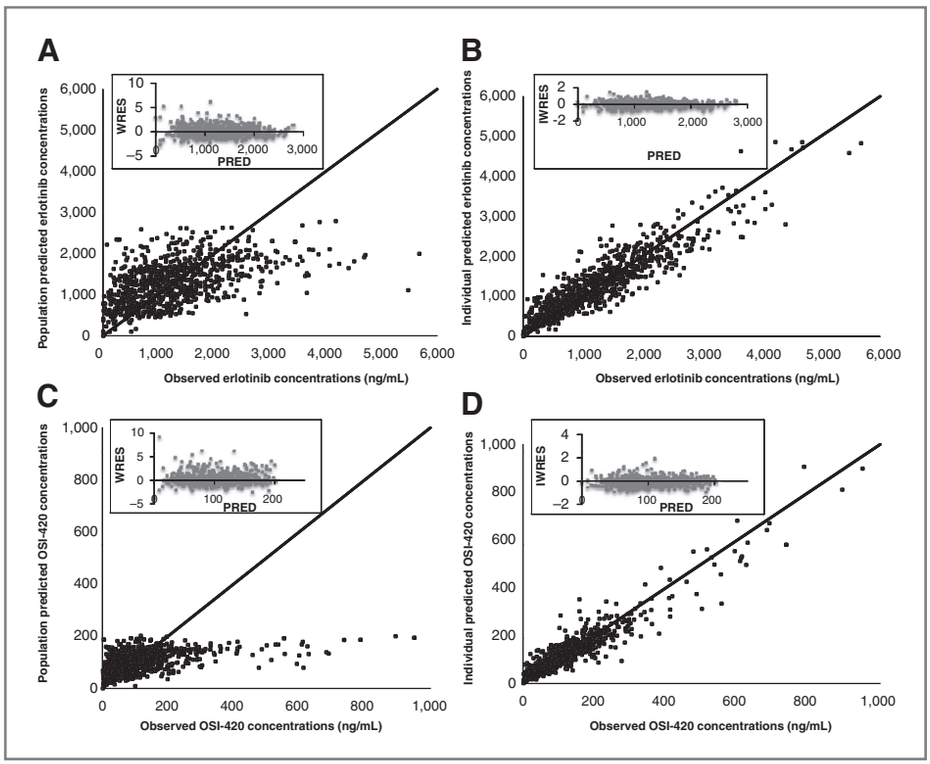

Figure 1. Goodness-of-fit plots for the final model. Plot of population (PRED) and individual (IPRED) predicted versus observed erlotinib (A and B) or OSI-420 (C and D) concentrations. Weighted residuals (WRES) and individual weighted residuals (IWRES) versus PRED are shown in insert.

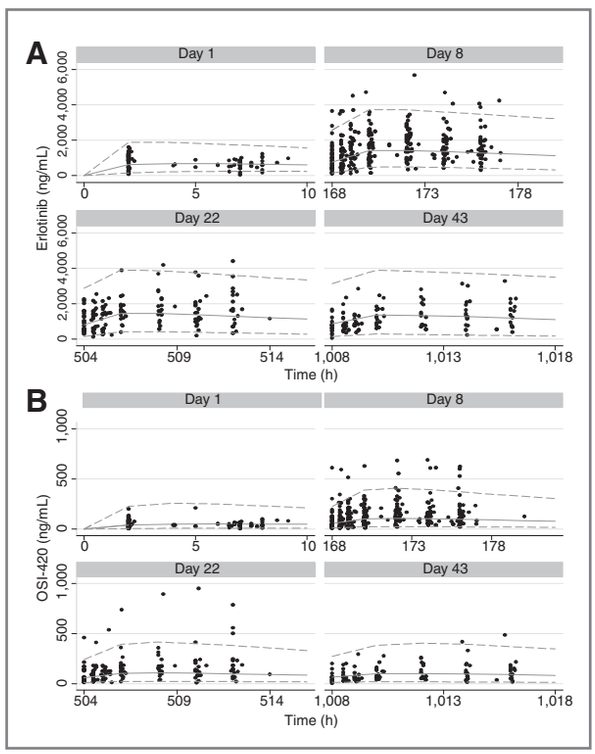

Figure 2. Visual predictive check of the final population model for erlotinib (A) and OSI-420 (B). Observed data are represented by points. The population-predicted profile (50th percentile) is shown by the solid line and the 90% prediction intervals by the broken lines.

trough erlotinib plasma levels observed at steady-state (data no shown).

Determination of a cutoff of erlotinib AUC

Using the ROC curve, the AUC threshold predicting a minimum skin toxicity of grade 2 was 27 ng·mL·h^{-1} with the area under the curve at 70% (CI 95% = [59%–81%], $P < 0.001$) in our population. The diagnostic accuracy values of sensitivity (SE) and specificity (SP) were 64.9% and 64.7%, respectively.

Discussion

Pharmacokinetic–pharmacodynamic (PK–PD) studies combining children and adults are scarce (29, 30). This PK–PD analysis carried out on data from two independent clinical trials contributes important information toward explaining the observed difference in erlotinib tolerance between pediatric and adult patients (i.e., daily recommended dose of 125 mg/m^2 vs. 150 mg corresponding to approximately 90 mg/m^2, respectively).

Although the skin symptoms were rather different between children and adults, the relationship between daily erlotinib AUC and the probability of skin toxicity was very consistent between the two subgroups. Previous phase I studies in children concluded that erlotinib and OSI-420 pharmacokinetics values were similar to those in adults (11, 31). However, in our study significant differences in pharmacokinetics were observed between children

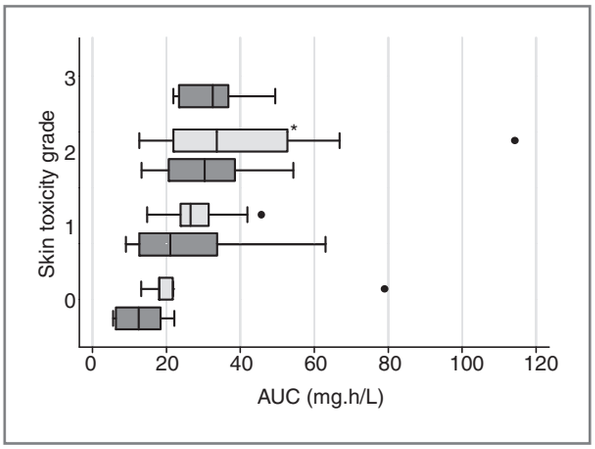

Figure 3. Box plot of severity of skin rash versus erlotinib exposure (AUC) both in adults (black box plot) and children (grey box plot). * the children in this box had grade 2 or 3 toxicity.

and adults. By considering the covariate POP (i.e., POP = 1 for children or POP = 0 for adults) alone or in combination with other covariates, the population approach applied to this dataset revealed and quantified this difference. A higher mean value of erlotinib clearance (i.e., + 54%) was observed in children compared with adults when expressed in $L{\cdot}h^{-1}{\cdot}kg^{-1}$. Comparison of the individual POSTHOC values confirmed this higher elimination capacity in children: CL = 0.146 ± 0.070 $L{\cdot}h^{-1}{\cdot}kg^{-1}$ for children versus CL = 0.095 ± 0.045 $L{\cdot}h^{-1}{\cdot}kg^{-1}$for adults. This pharmacokinetic particularity explains why the recommended dose in children is higher than in adults. The lack of data prevented us from including smoking status as a covariate in our study. However, a large proportion of the adults smoked (55%) whereas one can assume most of the children did not, which makes the higher clearance in children particularly remarkable and unexpected, as one can assume that the adults' clearance is increased due to the large proportion of smokers in that population. Specific consideration of the adolescents showed that their mean erlotinib clearance was lower than that in children younger than 12 years old, and was similar to that in adults. However, it is interesting to note that by adding the covariate POP to the final covariate model (i.e., which included body weight, ALAT, *CYP3A5*, and *ABCB1* (*2677*G>T/A)), the typical value of CL was only 11% higher in pediatrics (versus 24% when only the POP covariate is considered). This result showed that the final covariate model explains most of the difference between the two subgroups.

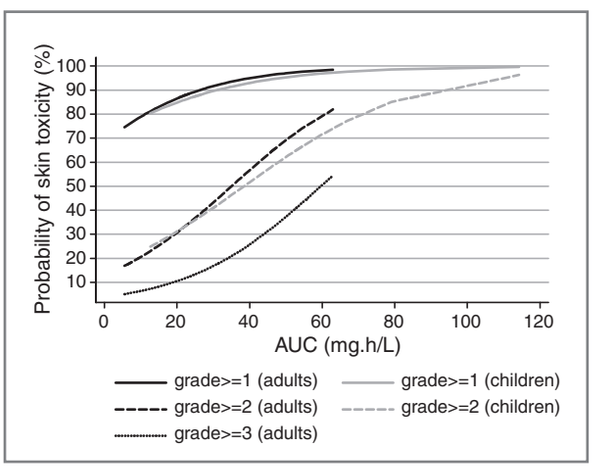

Figure 4. Relationship between skin toxicity and drug exposure (AUC) both in adults (black curves) and in children (grey curves). Curves show the cumulative probability (%) of having skin toxicity greater than or equal to a certain grade according to AUC, using the probabilities predicted by the four-level (for adults) and three-level (for children) ordered logistic regression model.

The erlotinib and OSI-420 clearance were negatively correlated with ALAT. An increase of this covariate might be the reflection of hepatic dysfunction, which leads to a decrease in erlotinib and OSI-420 clearance. The impact of hepatic dysfunction on erlotinib clearance has been confirmed in a clinical study using a more conventional approach (32).

Our results also highlight the relevance of taking into account pharmacogenetic information for erlotinib pharmacokinetics analysis. By analyzing children and adults together, we found that carriers of at least one allele **1* of *CYP3A5* had a 1.4 times higher clearance than patients harboring the *CYP3A5 *3/*3* genotype (which represents about 80% in Caucasians (33)). This observation is in agreement with the functional consequence of the *6986*G > A SNP (allele *CYP3A5*3*), which encodes an aberrantly spliced mRNA with a premature stop codon, leading to the absence of the protein (34). A similar trend was observed for *ABCB1 2677* G>T/A SNP. Although a recent work suggested that OSI-420, but not erlotinib, is a substrate for *ABCB1* (35), the presence of one variant allele (T or A) was associated with an average 20% decrease of the clearance of both erlotinib and OSI-420, suggesting the role of *ABCB1* in erlotinib elimination as described in another study (36).

These results confirm the relationship between plasma concentrations of tyrosine kinase inhibitors and their dose limiting toxicity. Besides, it has been suggested that patients experiencing skin rash during erlotinib treatment have an improved survival and rash has been proposed as a surrogate marker for favorable outcome (37). The correlation observed between exposure and rash in both adults and children and the previously observed relationship between rash and efficacy strongly supports the existence of an exposure/response correlation in addition to efficacy observed in EGFR amplified and mutant tumours (38, 39). There is now a need to evaluate the benefit of therapeutic drug monitoring in patients treated with erlotinib. The methodology we used here, consisting in AUC calculation from pharmacokinetic data processed with population pharmacokinetics followed by a ROC analysis to determine the cutoff AUC, is a reasonable approach. Due to the heterogeneity between patients in terms of disease, it was not possible

to examine the relationship between AUC and clinical response. Because previous clinical studies conducted with erlotinib in lung and pancreas cancer showed that a grade 2 rash was associated with a better outcome (37), we chose to determine the cutoff AUC associated with a grade 2 rash which is a surrogate marker for efficacy. In this study, we found a cutoff AUC of 27 ng/ml/h but further studies with larger datasets and in other groups of patients treated with erlotinib (e.g., lung-cancer patients) are necessary to determine optimal cutoff values and subsequently suggest their use in prospective clinical studies.

In conclusion, this analysis of combined data from two clinical trials showed that the higher recommended dose in children (125 mg/m^2/day) than in adults (90 mg/m^2/day) is mainly due to pharmacokinetic rather than pharmacodynamic particularities.

Disclosure of Potential Conflicts of Interest

No potential conflicts of interest were disclosed.

Acknowledgments

We thank all the patients and parents who participated in the trials, and the clinical teams of the centers (Institut Gustave Roussy, Villejuif, Centre Leon-Berard, Lyon, Institut Curie, Paris, Centre Oscar-Lambret, Lille, Royal Marsden Hospital, Sutton, CHU LaTimone, Marseille, Birmingham Children's Hospital, Birmingham, Catholic Gemelli University, Rome).

The costs of publication of this article were defrayed in part by the payment of page charges. This article must therefore be hereby marked *advertisement* in accordance with 18 U.S.C. Section 1734 solely to indicate this fact.

Received December 10, 2010; revised April 21, 2011; accepted May 19, 2011; published OnlineFirst June 8, 2011.

References

1. Li J, Zhao M, He P, Hidalgo M, Baker SD. Differential metabolism of gefitinib and erlotinib by human cytochrome P450 enzymes. Clin Cancer Res 2007;13:3731–7.
2. Ling J, Johnson KA, Miao Z, Rakhit A, Pantze MP, Hamilton M, et al. Metabolism and excretion of erlotinib, a small molecule inhibitor of epidermal growth factor receptor tyrosine kinase, in healthy male volunteers. Drug Metabol Dispos: Biol Fate Chem 2006;34:420–6.
3. Li J, Cusatis G, Brahmer J, Sparreboom A, Robey RW, Bates SE, et al. Association of variant ABCG2 and the pharmacokinetics of epidermal growth factor receptor tyrosine kinase inhibitors in cancer patients. Cancer Biol Ther 2007;6:432–8.
4. Shi Z, Peng XX, Kim IW, Shukla S, Si QS, Robey RW, et al. Erlotinib (Tarceva, OSI-774) antagonizes ATP-binding cassette subfamily B member 1 and ATP-binding cassette subfamily G member 2-mediated drug resistance. Cancer Res 2007;67:11012–20.
5. Johnson JR, Cohen M, Sridhara R, Chen YF, Williams GM, Duan J, et al. Approval summary for erlotinib for treatment of patients with locally advanced or metastatic non-small cell lung cancer after failure of at least one prior chemotherapy regimen. Clin Cancer Res 2005;11:6414–21.
6. Moore MJ, Goldstein D, Hamm J, Figer A, Hecht JR, Gallinger S, et al. Erlotinib plus gemcitabine compared with gemcitabine alone in patients with advanced pancreatic cancer: a phase III trial of the National Cancer Institute of Canada Clinical Trials Group. J Clin Oncol 2007;25:1960–6.
7. Geoerger B, Gaspar N, Opolon P, Morizet J, Devanz P, Lecluse Y, et al. EGFR tyrosine kinase inhibition radiosensitizes and induces apoptosis in malignant glioma and childhood ependymoma xenografts. Int J Cancer 2008;123:209–16.
8. Sarkaria JN, Yang L, Grogan PT, Kitange GJ, Carlson BL, Schroeder MA, et al. Identification of molecular characteristics correlated with glioblastoma sensitivity to EGFR kinase inhibition through use of an intracranial xenograft test panel. Mol Cancer Ther 2007;6:1167–74.
9. Broniscer A, Panetta JC, O'Shaughnessy M, Fraga C, Bai F, Krasin MJ, et al. Plasma and cerebrospinal fluid pharmacokinetics of erlotinib and its active metabolite OSI-420. Clin Cancer Res 2007;13:1511–5.
10. Jakacki RI, Hamilton M, Gilbertson RJ, Blaney SM, Tersak J, Krailo MD, et al. Pediatric phase I and pharmacokinetic study of erlotinib followed by the combination of erlotinib and temozolomide: a Children's Oncology Group Phase I Consortium Study. J Clin Oncol 2008;26:4921–7.
11. Broniscer A, Baker SJ, Stewart CF, Merchant TE, Laningham FH, Schaiquevich P, et al. Phase I and pharmacokinetic studies of erlotinib administered concurrently with radiotherapy for children, adolescents, and young adults with high-grade glioma. Clin Cancer Res 2009;15:701–7.
12. Geoerger B, Hargrave D, Thomas F, Ndiaye A, Frappaz D, Andreiuolo F, et al. Innovative Therapies for Children with Cancer pediatric phase I study of erlotinib in brainstem glioma and relapsing/refractory brain tumors. Neuro-oncology 2010.
13. Debiec-Rychter M, Sciot R, Le Cesne A, Schlemmer M, Hohenberger P, van Oosterom AT, et al. KIT mutations and dose selection for imatinib in patients with advanced gastrointestinal stromal tumours. Eur J Cancer 2006;42:1093–103.
14. Delbaldo C, Chatelut E, Re M, Deroussent A, Seronie-Vivien S, Jambu A, et al. Pharmacokinetic-pharmacodynamic relationships of imatinib and its main metabolite in patients with advanced gastrointestinal stromal tumors. Clin Cancer Res 2006;12:6073–8.
15. Larson RA, Druker BJ, Guilhot F, O'Brien SG, Riviere GJ, Krahnke T, et al. Imatinib pharmacokinetics and its correlation with response and safety in chronic-phase chronic myeloid leukemia: a subanalysis of the IRIS study. Blood 2008;111:4022–8.
16. Picard S, Titier K, Etienne G, Teilhet E, Ducint D, Bernard MA, et al. Trough imatinib plasma levels are associated with both cytogenetic and molecular responses to standard-dose imatinib in chronic myeloid leukemia. Blood 2007;109:3496–9.
17. Demetri GD, Wang Y, Wehrle E, Racine A, Nikolova Z, Blanke CD, et al. Imatinib plasma levels are correlated with clinical benefit in patients with unresectable/metastatic gastrointestinal stromal tumors. J Clin Oncol 2009;27:3141–7.
18. Widmer N, Decosterd LA, Leyvraz S, Duchosal MA, Rosselet A, Debiec-Rychter M, et al. Relationship of imatinib-free plasma levels and target genotype with efficacy and tolerability. Br J Cancer 2008;98:1633–40.
19. Houk BE, Bello CL, Poland B, Rosen LS, Demetri GD, Motzer RJ. Relationship between exposure to sunitinib and efficacy and tolerability endpoints in patients with cancer: results of a pharmacokinetic/pharmacodynamic meta-analysis. Cancer Chemother Pharmacol 2010;66:357–71.
20. Thomas F, Rochaix P, Benlyazid A, Sarini J, Rives M, Lefebvre JL, et al. Pilot study of neoadjuvant treatment with erlotinib in nonmetastatic head and neck squamous cell carcinoma. Clin Cancer Res 2007;13:7086–92.
21. Thomas F, Rochaix P, White-Koning M, Hennebelle I, Sarini J, Benlyazid A, et al. Population pharmacokinetics of erlotinib and its pharmacokinetic/pharmacodynamic relationships in head and neck squamous cell carcinoma. Eur J Cancer 2009;45:2316–23.
22. Smith M, Bernstein M, Bleyer WA, Borsi JD, Ho P, Lewis IJ, et al. Conduct of phase I trials in children with cancer. J Clin Oncol 1998;16:966–78.

23. Ivanova A. Dose finding in oncology–non-parametric methods. New York, NY: 2006.
24. O'Quigley J, Shen LZ. Continual reassessment method: a likelihood approach. Biometrics 1996;52:673–84.
25. Zhao M, He P, Rudek MA, Hidalgo M, Baker SD. Specific method for determination of OSI-774 and its metabolite OSI-420 in human plasma by using liquid chromatography-tandem mass spectrometry. J Chromatogr 2003;793:413–20.
26. Cascorbi I, Gerloff T, Johne A, Meisel C, Hoffmeyer S, Schwab M, et al. Frequency of single nucleotide polymorphisms in the P-glycoprotein drug transporter MDR1 gene in white subjects. Clin Pharmacol Ther 2001;69:169–74.
27. Asano T, Takahashi KA, Fujioka M, Inoue S, Okamoto M, Sugioka N, et al. ABCB1 C3435T and G2677T/A polymorphism decreased the risk for steroid-induced osteonecrosis of the femoral head after kidney transplantation. Pharmacogenetics 2003;13:675–82.
28. Yates CR, Zhang W, Song P, Li S, Gaber AO, Kotb M, et al. The effect of CYP3A5 and MDR1 polymorphic expression on cyclosporine oral disposition in renal transplant patients. J Clin Pharmacol 2003; 43:555–64.
29. Petain A, Kattygnarath D, Azard J, Chatelut E, Delbaldo C, Geoerger B, et al. Population pharmacokinetics and pharmacogenetics of imatinib in children and adults. Clin Cancer Res 2008;14:7102–9.
30. Tod M, Jullien V, Pons G. Facilitation of drug evaluation in children by population methods and modelling. Clin Pharmacokinetics 2008; 47:231–43.
31. Christiansen SR, Broniscer A, Panetta JC, Stewart CF. Pharmacokinetics of erlotinib for the treatment of high-grade glioma in a pediatric patient with cystic fibrosis: case report and review of the literature. Pharmacotherapy 2009;29:858–66.
32. Miller AA, Murry DJ, Owzar K, Hollis DR, Lewis LD, Kindler HL, et al. Phase I and pharmacokinetic study of erlotinib for solid tumors in patients with hepatic or renal dysfunction: CALGB 60101. J Clin Oncol 2007;25:3055–60.
33. VanSchaik RHN. CYP3A5 variant allele frequencies in Dutch Caucasians. Clin Chem 2002;48:1668–71.
34. Kuehl P, Zhang J, Lin Y, Lamba J, Assem M, Schuetz J, et al. Sequence diversity in CYP3A promoters and characterization of the genetic basis of polymorphic CYP3A5 expression. Nat Genet 2001;27:383–91.
35. Elmeliegy MA, Carcaboso AM, Tagen M, Bai F, Stewart CF. Role of ATP-binding cassette and solute carrier transporters in erlotinib CNS penetration and intracellular accumulation. Clin Cancer Res 17;89–99.
36. Marchetti S, de Vries NA, Buckle T, Bolijn MJ, van Eijndhoven MA, Beijnen JH, et al. Effect of the ATP-binding cassette drug transporters ABCB1, ABCG2, and ABCC2 on erlotinib hydrochloride (Tarceva) disposition in in vitro and in vivo pharmacokinetic studies employing Bcrp1-/-/Mdr1a/1b-/- (triple-knockout) and wild-type mice. Mol Cancer Ther 2008;7:2280–7.
37. Wacker B, Nagrani T, Weinberg J, Witt K, Clark G, Cagnoni PJ. Correlation between development of rash and efficacy in patients treated with the epidermal growth factor receptor tyrosine kinase inhibitor erlotinib in two large phase III studies. Clin Cancer Res 2007;13:3913–21.
38. Mellinghoff IK, Wang MY, Vivanco I, Haas-Kogan DA, Zhu S, Dia EQ, et al. Molecular determinants of the response of glioblastomas to EGFR kinase inhibitors. New Engl J Med 2005;353:2012–24.
39. Lynch TJ, Bell DW, Sordella R, Gurubhagavatula S, Okimoto RA, Brannigan BW, et al. Activating mutations in the epidermal growth factor receptor underlying responsiveness of non-small-cell lung cancer to gefitinib. N Engl J Med 2004;350:2129–39.